# Input Admittance of a Multilayer Insulated Monopole Antenna

Zhongxiang Shen, *Student Member, IEEE,* and Robert H. MacPhie, *Fellow, IEEE*

***Abstract*—An efficient numerical technique based on the modal-expansion method in conjunction with a recursive algorithm is developed for a multilayer insulated monopole antenna fed by a coaxial transmission line. The modal-expansion analysis is facilitated by introducing a perfectly matched boundary (PMB) at a variable height over the ground plane of the monopole. The current distribution and input admittance are computed by finding the expansion coefficients of the electromagnetic field expressions. Numerical results for the input admittance of a dielectric-coated monopole antenna and an air-insulated monopole are compared with experimental ones available in the literature. Good agreement is achieved. Calculated results for the effects of various parameters on the input admittance of an air-insulated monopole antenna are presented and discussed.**

***Index Terms*—Monopole antennas.**

## I. Introduction

INSULATED antennas have found wide applications in subsurface communication, geophysical exploration, and biomedical telemetry [1], [2]. An insulated linear antenna consists of a metal wire enclosed in a cylinder that is usually composed of a low-loss dielectric material. Considerable theoretical and experimental investigations of the insulated antenna have been performed by King *et al*. [1]–[7]. Unfortunately, much of their work is restricted to the case where the complex permittivity of the exterior medium is much greater than that of the insulating layer. Lee [2], [7] extended the applicable range of the transmission-line solution based on a complicated formulation. Furthermore, most attention of the previous work was focused on the current and charge distributions along the insulated antenna.

Another similar problem of a monopole/dipole antenna coated with a dielectric layer has also attracted some attention [8]–[11]. An important experimental investigation was carried out by Lamensdorf [8]. Several theoretical analysis techniques such as the integral equation technique [9], the moment method [10], and the Wiener–Hopf technique [11] were reported in the past decades. The present paper deals with the general case of a multilayer insulated monopole antenna including both the dielectric-coated monopole and the air-insulated monopole antenna as its special cases.

Recently, an efficient modal-expansion method was developed for the analysis of monopole antennas fed through an infinite ground plane by a coaxial line [12] and the sleeve monopole antenna [13]. The modal-expansion analysis is facilitated by the introduction of a perfectly matched boundary (PMB), which is the combination of an electrical wall and a magnetic wall [13] above the monopole and parallel to the ground plane [14]. The introduced PMB is expected to have little effect on the antenna's current distribution and input admittance since the main radiation of the insulated monopole occurs in the horizontal direction [1]. The resulting guided-wave structure is then divided into several subregions; the electromagnetic fields in these subregions are expressed by the summation of their modal functions weighted by unknown expansion coefficients. These coefficients, which ultimately yield the current distribution and input admittance of the antenna, are found by enforcing the boundary and continuity conditions at conducting surfaces and regional interfaces. An efficient recursive algorithm based on $2 \times 2$ matrix multiplications is presented to implement the analysis of an arbitrary multilayer insulated monopole antenna. The modal-expansion method presented in the paper not only rigorously takes the effect of the coaxial feed line into account, but is also valid for the cases of a thick monopole antenna and a monopole immersed in a multilayer dielectric cylinder of arbitrary permittivities.

Section II begins with a description of the theoretical model for a multilayer insulated monopole. Then a general formulation of the modal expansion analysis of an $N$-layer insulated monopole antenna will be introduced. As illustrative numerical examples, a dielectric-coated monopole and an air-insulated monopole antenna in a medium such as water and/or sand are considered in Section III. The calculated input admittance of these antenna structures is in good agreement with the experimental one measured by Lamensdorf [8] and Lee *et al*. [2], [7]. Also in Section III the effect of the step discontinuity at the base of the monopole is examined.

## II. Formulation

### A. Description of the Model

The theoretical model we employ to characterize an $N$-layer insulated monopole antenna fed by a coaxial transmission line is shown in Fig. 1, where a perfectly matched boundary (PMB) [13] is placed parallel to the ground plane at a distance $d$ above the monopole. Due to the nonreflecting property of the PMB we actually assume that the height of all the cylindrical dielectric layers is infinite. This is a very good assumption since the main radiation of the monopole antenna occurs in

Manuscript received October 10, 1996; revised August 18, 1997. This work was supported by the Natural Sciences and Engineering Research Council (NSERC) of Canada under Grant 0GP0002176.

The authors are with the Department of Electrical and Computer Engineering, University of Waterloo, Waterloo, ON, N2L 3G1 Canada.

Publisher Item Identifier S 0018-926X(98)08889-9.

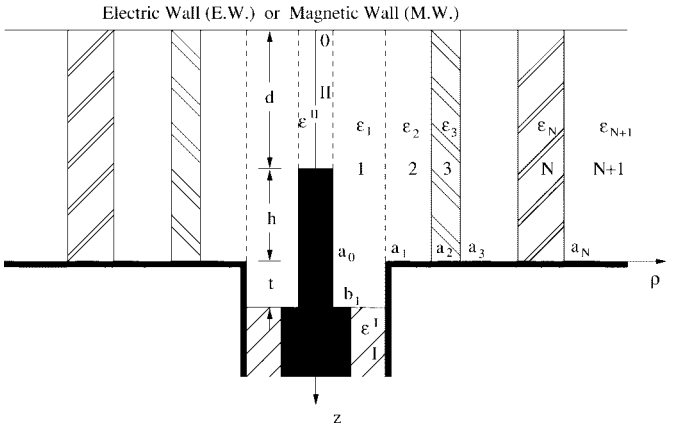


Fig. 1. Theoretical model of a multilayer insulated monopole antenna fed by a coaxial line.

the radial direction and the radiation is null in the $z$ direction. Therefore, the truncation of the dielectric layer after a certain distance (more than one free-space wavelength) does not have much influence on the antenna's performance, as seen from the numerical examples given in the next section.

There is a step junction between the monopole and the coaxial feed line [6], as shown in Fig. 1. The inner and outer radii of the coaxial feed line are $b_1$ and $a_1$, respectively, while the radius of the monopole antenna is $a_0$ ($a_0 \le b_1$). The analysis of the $N$-layer insulated monopole requires the solution of the two problems: one with a parallel electric wall and the other with a parallel magnetic wall over the monopole; they are both solved by the modal expansion method. The reflection coefficient at the feed point, which is related to the antenna's input admittance, is then obtained by halving the sum of these two results. Since the formulation for the case of the electric wall is very similar to that of the magnetic wall, we will only briefly give the formulation for the magnetic wall in the following. As illustrated in Fig. 1, the whole structure of interest is divided into $(N+3)$ subregions: I, II, 1, 2, $\cdots$, $N$ and $N+1$. Since the structure and the incident dominant TEM mode in the coaxial feed waveguide are axisymmetric (no $\phi$ variation), only three field components ($E_z$, $E_\rho$, and $H_\phi$) are nonzero.

### B. Field Component Expressions

The electromagnetic field components in Regions I and II are given [12], [13] as follows.

*Region I:*

$$E_\rho^I = \sum_{n=1}^{N_1} (A_{In}\exp[j\beta_{In}(z-L)] + A_{Rn}\exp[-j\beta_{In}(z-L)])e_{In\rho} \tag{1a}$$

$$H_\phi^I = \sum_{n=1}^{N_1} (-A_{In}\exp[j\beta_{In}(z-L)] + A_{Rn}\exp[-j\beta_{In}(z-L)])Y_{In}e_{In\rho} \tag{1b}$$

where $L = d+h+t$, $\mathbf{A}_{In} = (A_{I1}, A_{I2}, \cdots, A_{IN_1})^T$, and $\mathbf{A}_{Rn} = (A_{R1}, A_{R2}, \cdots, A_{RN_1})^T$, with $T$ representing the transpose operation, are the incident and reflected modal-amplitude column vectors in the coaxial feed waveguide; $\beta_{In} = \sqrt{k_0^2\epsilon_r^I - (x_{In}/b_1)^2}$ with $(x_{In}/b_1)$ being the cutoff wavenumber of the $n$th mode and $Y_{In}$ are, respectively, its propagation constant and modal admittance. The expression for the normalized transverse modal electric field $e_{In\rho}$ is given in [15].

*Region II:*

$$E_z^{II} = \sum_{n=0}^{N_2} \frac{2A_n^{II}}{j\omega\epsilon^{II}d}\sin\frac{(2n+1)\pi z}{2d}\frac{\gamma_n^{II}J_0(\gamma_n^{II}\rho)}{J_1(\gamma_n^{II}a_0)} \tag{2a}$$

$$E_\rho^{II} = \sum_{n=1}^{N_2} \frac{-(2n+1)\pi A_n^{II}}{j\omega\epsilon^{II}d^2}\cos\frac{(2n+1)\pi z}{2d}\frac{J_1(\gamma_n^{II}\rho)}{J_1(\gamma_n^{II}a_0)} \tag{2b}$$

$$H_\phi^{II} = \sum_{n=0}^{N_2} \frac{2A_n^{II}}{d}\sin\frac{(2n+1)\pi z}{2d}\frac{J_1(\gamma_n^{II}\rho)}{J_1(\gamma_n^{II}a_0)} \tag{2c}$$

where $(\gamma_n^{II})^2 = k_0^2\epsilon_r^{II} - [(2n+1)\pi/d]^2$, $J_0$, and $J_1$ are the first kind Bessel functions of order zero and one, respectively. $A_n^{II}$ is the expansion coefficient to be determined.

The expressions for the electromagnetic fields in Region 1 can be obtained by employing the resonator method [16].

$$E_z^1 = \frac{1}{j\omega\epsilon_1}\left(\sum_{n=0}^{N_3}[U_{1n}(\rho)A_{1n} + V_{1n}(\rho)B_{1n}]\sin\frac{(2n+1)\pi z}{2L} - \sum_{n=1}^{N_1'} C_n e_{1nz}(\rho)\frac{\sin(\alpha_n z)}{\alpha_n\cos(\alpha_n L)}\right) \tag{3a}$$

$$E_\rho^1 = \sum_{n=0}^{N_3}\frac{(2n+1)\pi}{j2\omega\epsilon_1 L\gamma_{1n}^2}[U_{1n}'(\rho)A_{1n} + V_{1n}'(\rho)B_{1n}] \times\cos\frac{(2n+1)\pi z}{2L} + \sum_{n=1}^{N_1'}\frac{C_n e_{1n\rho}(\rho)}{j\omega\epsilon_1}\frac{\cos(\alpha_n z)}{\cos(\alpha_n L)} \tag{3b}$$

$$H_\phi^1 = \sum_{n=0}^{N_3}\frac{-1}{\gamma_{1n}^2}[U_{1n}'(\rho)A_{1n} + V_{1n}'(\rho)B_{1n}]\sin\frac{(2n+1)\pi z}{2L} - \sum_{n=1}^{N_1'} C_n e_{1n\rho}(\rho)\frac{\sin(\alpha_n z)}{\alpha_n\cos(\alpha_n L)} \tag{3c}$$

where $e_{1nz}(\rho)$ and $e_{1n\rho}(\rho)$ are the longitudinal and transverse electric field components [15] in a coaxial waveguide whose inner and outer radii are $a_0$ and $a_1$, respectively; $\alpha_n = \sqrt{k_0^2\epsilon_r^1 - (x_n'/a_0)^2}$ with $(x_n'/a_0)$ being the cutoff wavenumber of the $n$th mode in that waveguide

$$\gamma_{in}^2 = \begin{cases} k_0^2\epsilon_{ri} - [(2n+1)\pi/2L]^2, & \text{for } i=1 \\ k_0^2\epsilon_{ri} - [(2n+1)\pi/2D]^2, & \text{for } i = 2,\cdots, \text{ and } N+1 \end{cases}$$

with $D = d+h$ and

$$U_{in}(\rho) = \frac{J_0(\gamma_{in}\rho)Y_0(\gamma_{in}a_{i-1}) - Y_0(\gamma_{in}\rho)J_0(\gamma_{in}a_{i-1})}{J_0(\gamma_{in}a_i)Y_0(\gamma_{in}a_{i-1}) - Y_0(\gamma_{in}a_i)J_0(\gamma_{in}a_{i-1})}$$

$$V_{in}(\rho) = \frac{J_0(\gamma_{in}a_i)Y_0(\gamma_{in}\rho) - Y_0(\gamma_{in}a_i)J_0(\gamma_{in}\rho)}{J_0(\gamma_{in}a_i)Y_0(\gamma_{in}a_{i-1}) - Y_0(\gamma_{in}a_i)J_0(\gamma_{in}a_{i-1})}.$$

for $i = 1, 2, \cdots, N$. The electromagnetic fields in Region $i$ $(i = 2, 3, \cdots, N)$ are as follows:

$$E_z^i = \frac{1}{j\omega\epsilon_i}\sum_{n=0}^{N_4}[U_{in}(\rho)A_{in} + V_{in}(\rho)B_{in}]\sin\frac{(2n+1)\pi z}{2D} \tag{4a}$$

$$E_\rho^i = \sum_{n=0}^{N_4}\frac{(2n+1)\pi}{j2\omega\epsilon_i D\gamma_{in}^2}[U'_{in}(\rho)A_{in} + V'_{in}(\rho)B_{in}] \times\cos\frac{(2n+1)\pi z}{2D} \tag{4b}$$

$$H_\phi^i = \sum_{n=0}^{N_4}\frac{-1}{\gamma_{in}^2}[U'_{in}(\rho)A_{in} + V'_{in}(\rho)B_{in}]\sin\frac{(2n+1)\pi z}{2D}. \tag{4c}$$

Finally, the electromagnetic field components in Region $N+1$ have the form of

$$E_z^{N+1} = \sum_{n=0}^{N_4}\frac{A_{(N+1)n}}{j\omega\epsilon_{N+1}}\sin\frac{(2n+1)\pi z}{2D}\frac{H_0^{(2)}(\gamma_{(N+1)n}\rho)}{H_0^{(2)}(\gamma_{(N+1)n}a_N)} \tag{5a}$$

$$E_\rho^{N+1} = \sum_{n=0}^{N_4}\frac{-(2n+1)\pi A_{(N+1)n}}{j2\omega\epsilon_{N+1}D}\cos\frac{(2n+1)\pi z}{2D} \times\frac{H_1^{(2)}(\gamma_{(N+1)n}\rho)}{\gamma_{(N+1)n}H_0^{(2)}(\gamma_{(N+1)n}a_N)} \tag{5b}$$

$$H_\phi^{N+1} = \sum_{n=0}^{N_4}A_{(N+1)n}\sin\frac{(2n+1)\pi z}{2D} \times\frac{H_1^{(2)}(\gamma_{(N+1)n}\rho)}{\gamma_{(N+1)n}H_0^{(2)}(\gamma_{(N+1)n}a_N)} \tag{5c}$$

where $H_0^{(2)}$ and $H_1^{(2)}$ are the outgoing second kind Hankel functions of order zero and one, respectively.

### C. Application of Boundary Conditions

The boundary conditions that the tangential electromagnetic fields must be continuous at the interface $\rho = a_N$ result in

$$A_{(N+1)n} = \frac{\epsilon_{N+1}}{\epsilon_N}A_{Nn} \tag{6a}$$

$$Y_{(N+1)n}A_{(N+1)n} = -U'_{Nn}(a_N)A_{Nn} - V'_{Nn}(a_N)B_{Nn} \tag{6b}$$

or, in matrix form,

$$\begin{bmatrix}A_{Nn}\\ B_{Nn}\end{bmatrix} = \begin{bmatrix}\epsilon_N/\epsilon_{N+1}\\ -\frac{Y_{(N+1)n}+\epsilon_N U'_{Nn}(a_N)/\epsilon_{N+1}}{V'_{Nn}(a_N)}\end{bmatrix}A_{(N+1)n} \tag{6′}$$

where

$$Y_{(N+1)n} = \frac{\gamma_{Nn}^2 H_1^{(2)}(\gamma_{(N+1)n}a_N)}{\gamma_{(N+1)n}H_0^{(2)}(\gamma_{(N+1)n}a_N)}.$$

Enforcement of the continuity conditions of tangential electromagnetic fields at the interface $\rho = a_i$ $(i = 2, 3, \cdots, N-1)$ leads to

$$\frac{A_{in}}{\epsilon_i} = \frac{B_{(i+1)n}}{\epsilon_{i+1}} \tag{7a}$$

$$-\frac{U'_{in}(a_i)}{\gamma_{in}^2}A_{in} - \frac{V'_{in}(a_i)}{\gamma_{in}^2}B_{in} = -\frac{U'_{(i+1)n}(a_i)}{\gamma_{(i+1)n}^2}A_{(i+1)n} - \frac{V'_{(i+1)n}(a_i)}{\gamma_{(i+1)n}^2}B_{(i+1)n} \tag{7b}$$

or

$$\begin{bmatrix}A_{in}\\ B_{in}\end{bmatrix} = \mathbf{T}_i\begin{bmatrix}A_{(i+1)n}\\ B_{(i+1)n}\end{bmatrix} = \begin{bmatrix}0 & \epsilon_i/\epsilon_{i+1}\\ \frac{\gamma_{in}^2U'_{(i+1)n}(a_i)}{\gamma_{(i+1)n}^2V'_{in}(a_i)} & \frac{\gamma_{in}^2V'_{(i+1)n}(a_i)}{\gamma_{(i+1)n}^2V'_{in}(a_i)} - \frac{\epsilon_i U'_{in}(a_i)}{\epsilon_{i+1}V'_{in}(a_i)}\end{bmatrix} \times\begin{bmatrix}A_{(i+1)n}\\ B_{(i+1)n}\end{bmatrix}. \tag{7′}$$

Equation (7′) provides a recursive relation of the electromagnetic fields between two adjacent dielectric regions. Repeatedly using (7′) and taking (6′) into account, we can obtain

$$A_{2n} = R_{Tn}B_{2n} = \frac{T_{1n}^t}{T_{2n}^t}B_{2n} \tag{8}$$

where

$$\begin{bmatrix}T_{1n}^t\\ T_{2n}^t\end{bmatrix} = \mathbf{T}_2\mathbf{T}_3\cdots\mathbf{T}_{N-1}\begin{bmatrix}\epsilon_N/\epsilon_{N+1}\\ -\frac{Y_{(N+1)n}+\epsilon_N U'_{Nn}(a_N)/\epsilon_{N+1}}{V'_{Nn}(a_N)}\end{bmatrix}.$$

Application of the boundary conditions that the tangential electromagnetic field components must be continuous at the interfaces $\rho = a_0$, $\rho = a_1$, and $z = L$ leads to the following matrix equations:

$$\mathbf{B}_1 = \mathbf{W}_B\mathbf{A}^{II} = \mathbf{W}_B(\mathbf{M}_{2A}\mathbf{A}_1 + \mathbf{M}_{2B}\mathbf{B}_1 + \mathbf{M}_{2C}\mathbf{C}_1) \tag{9}$$

$$\mathbf{A}_1 = \mathbf{W}_A\mathbf{B}_2 \tag{10a}$$

$$\mathbf{Y}_A\mathbf{B}_2 = \mathbf{M}_{3A}\mathbf{A}_1 + \mathbf{M}_{3B}\mathbf{B}_1 + \mathbf{M}_{3C}\mathbf{C}_1 \tag{10b}$$

$$\mathbf{C}_1 = \mathbf{W}_C(\mathbf{A}_I + \mathbf{A}_R) \tag{11a}$$

$$\mathbf{Y}_I(\mathbf{A}_I - \mathbf{A}_R) = \mathbf{M}_{IA}\mathbf{A}_1 + \mathbf{M}_{IB}\mathbf{B}_1 + \mathbf{M}_{IC}\mathbf{C}_1 \tag{11b}$$

where the elements of all the above matrices are elucidated in the Appendix.

After some manipulations one has no difficulty in arriving at

$$\mathbf{A}_R = \left[2\left(\mathbf{I} - \mathbf{Y}_I^{-1}\mathbf{Y}_{L0}\right)^{-1} - \mathbf{I}\right]\mathbf{A}_I \tag{12}$$

where

$$\mathbf{Y}_{L0} = [(\mathbf{M}_{IA}\mathbf{Q}\mathbf{M}_{3B} + \mathbf{M}_{IB})\mathbf{Y}_M + \mathbf{M}_{IA}\mathbf{Q}\mathbf{M}_{3C} + \mathbf{M}_{IC}]\mathbf{W}_C$$

$$\mathbf{Y}_M = [\mathbf{I} - \mathbf{W}_B(\mathbf{M}_{2A}\mathbf{Q}\mathbf{M}_{3B} + \mathbf{M}_{2B})]^{-1} \times(\mathbf{M}_{2A}\mathbf{Q}\mathbf{M}_{3C} + \mathbf{M}_{2C})$$

with $\mathbf{Q} = (\mathbf{I} - \mathbf{W}_A\mathbf{Y}_A^{-1}\mathbf{M}_{3A})^{-1}\mathbf{W}_A\mathbf{Y}_A^{-1}$. From (12) we can obtain the reflection coefficients for all of the modes in the coaxial feed waveguide assuming the incident column vector $\mathbf{A}_I$ is known (for example, $(1, 0, \cdots, 0)^T$). Other expansion coefficients can be found from (9)–(11). Then the input admittance of the multilayer insulated monopole antenna and the current distribution along the monopole can be straightforwardly calculated by using the computed expansion coefficients. For detailed formulation, the reader is referred to [13].

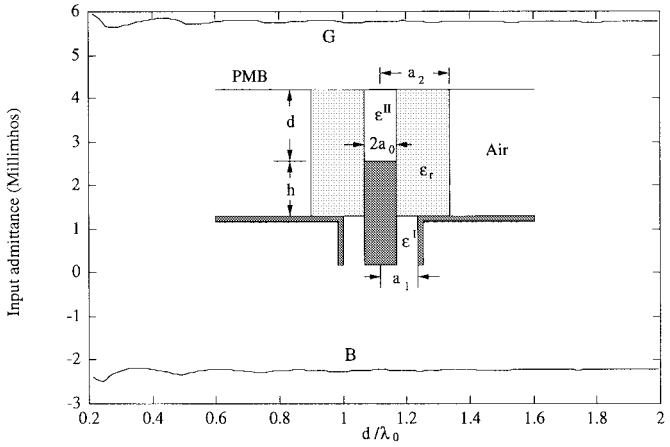


Fig. 2. Variation of the input admittance of a dielectric-coated monopole antenna with respect to the distance $d$ from the assumed PMB to the monopole end ($a_0 = 3.175$ mm, $a_1 = 3a_0$, $\epsilon_r^I = 1.735$, $a_2 = 11.43$ mm, $\epsilon_r = 3.2$, $\epsilon_r^{II} = 1$, $h = 0.25\lambda_0$, $f = 600$ MHz).

## III. Numerical Examples

This section gives some sample numerical results computed by our modal expansion method described in the preceding section. A check on the convergence behavior of the truncated numbers $N_1$, $N_1'$, $N_2$, $N_3$, $N_4$ for the field expansion expressions is performed initially. It is found that the choices of $N_1 = 2$, $N_1' = [(a_1 - a_0)/(a_1 - b_1)]N_1$, $N_2 = 80$, and $N_4 = (D/d)N_2$ [13], [17] are essential to provide convergent results for the numerical examples that follow.

### A. Dielectric-Coated Monopole

The first example is a dielectric-coated monopole antenna whose geometry is shown in Fig. 2. The effect of the assumed PMB on the input admittance of a dielectric-coated monopole antenna is initially examined, as shown in Fig. 2. It is seen that the effect is negligible when the distance $d$ from the PMB to the end of the monopole is greater than one free-space wavelength [13]. The choice of $d = \sqrt{2}\lambda_0$ is adopted in the later computations.

A comparison between our results and experimental ones in [8] is shown in Fig. 3 for the input admittance of a dielectric-coated monopole antenna. The agreement is quite good for both the conductance $G$ and the susceptance $B$. It is obvious that the monopole's resonant conductance increases and its resonant length decreases as the diameter of the dielectric coating increases. Similarly, increasing the dielectric constant of the coating cylinder decreases the antenna's resonant length and bandwidth. Moreover, with a large permittivity of the dielectric coating, our results for the input conductance $G$ of a monopole agree very well with the experimental data measured by Lamensdorf [8], while the agreement deteriorates for the antenna's susceptance $B$. A similar disagreement between the moment-method solution [10] and the measured data in [8] occurred for coating dielectrics with high permittivity or large diameter.

### B. Air-Insulated Monopole

Fig. 4 shows the geometry of an air-insulated monopole antenna. As with the dielectric-coated monopole, the effect of

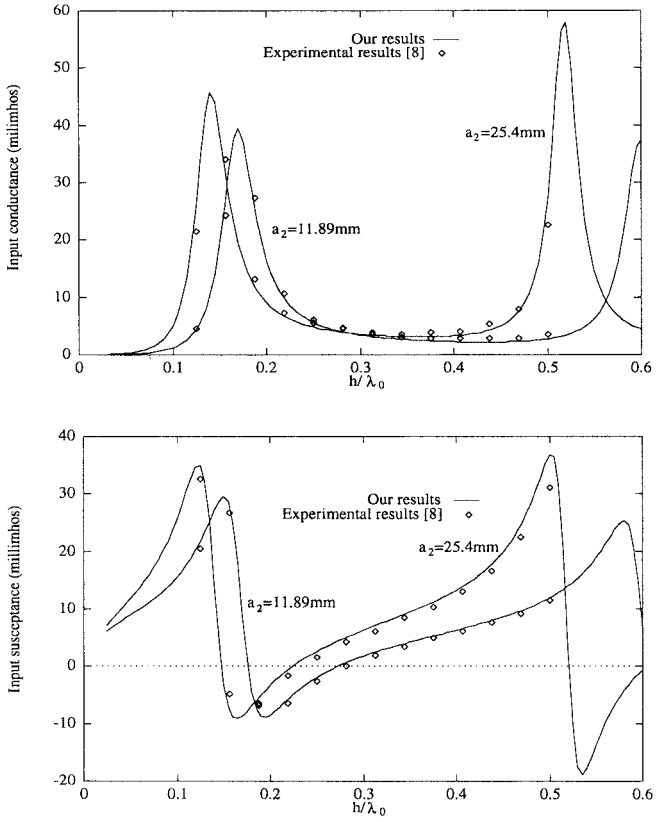


Fig. 3. Input admittance of a dielectric-coated monopole antenna (same parameters as in Fig. 2).

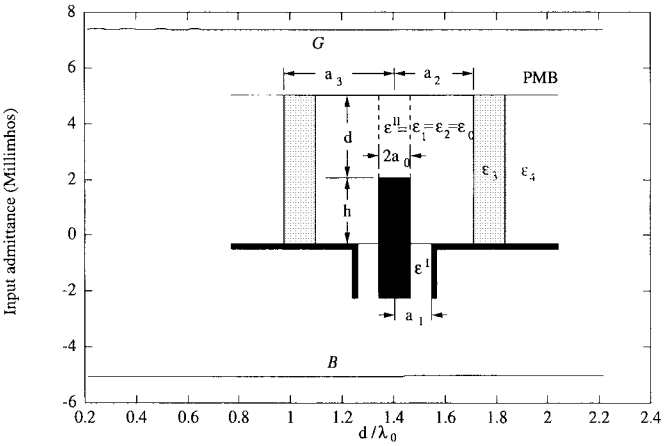


Fig. 4. Variation of the input admittance of an air-insulated monopole with respect to $d$ ($a_0 = 3.175$ mm, $a_1 = 3a_0$, $\epsilon_r^I = 1.735$, $a_2 = 4a_0$, $\epsilon_{r3} = 4.2$, $a_3 - a_2 = 0.1a_0$, $\epsilon_{r4} = 3.8$, $h = 0.25\lambda_0$, $f = 380$ MHz).

the assumed PMB on the input admittance of an air-insulated monopole is examined in Fig. 4. The effect is negligible even when the distance $d$ from the PMB to the end of the monopole is fairly small. Since more energy is stored in the external medium, the effect caused by the assumed PMB becomes weaker. The value $d = \sqrt{2}\lambda_0$ is also used for computing the results hereafter.

Figs. 5 and 6 illustrate the current distribution and input admittance of an air-insulated monopole antenna in sand; also given are the theoretical and experimental data obtained by

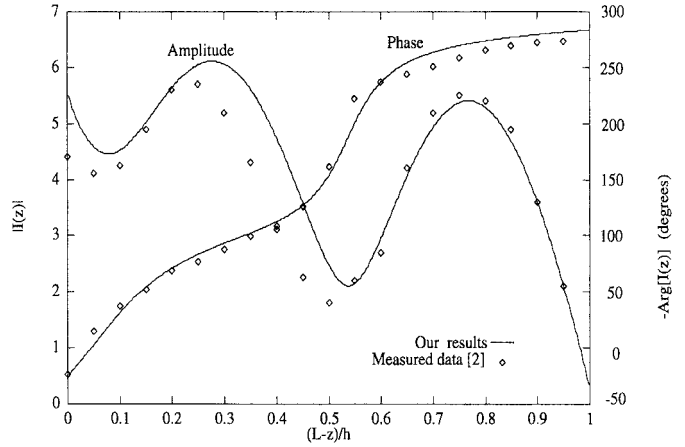


Fig. 5. Current distribution on an air-insulated monopole antenna in sand ($a_0 = 3.175$ mm, $a_1 = 3a_0$, $\epsilon_r^I = 1.735$, $a_2 = 4a_0$, $\epsilon_{r3} = 4.82$, $a_3 - a_2 = 0.1a_0$, $\epsilon_{r4} = 3.8$, $h = 0.765\lambda_0$, $f = 380$ MHz).

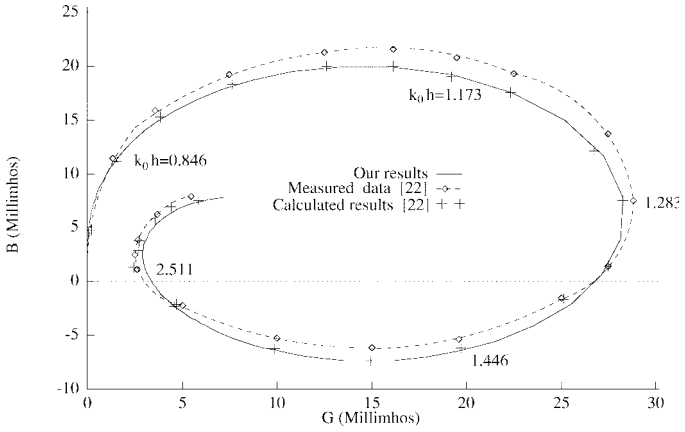


Fig. 6. Input admittance of an air-insulated monopole antenna in sand ($a_0 = 3.175$ mm, $a_1 = 3a_0$, $\epsilon_r^I = 1.735$, $a_2 = 4a_0$, $\epsilon_{r3} = 4.82$, $\epsilon_{r4} = 3.8$, $a_3 - a_2 = 0.1a_0$, $f = 380$ MHz).

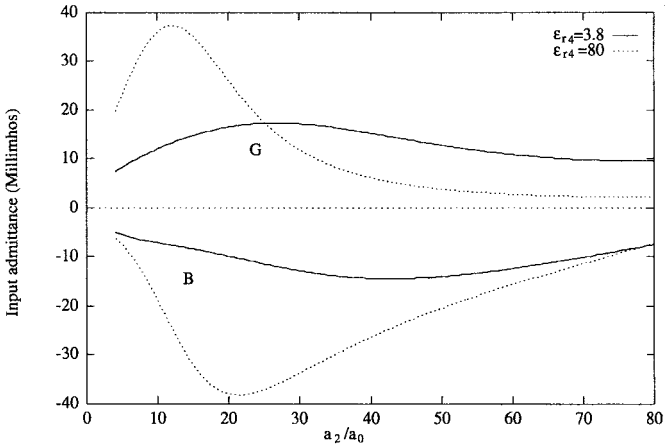


Fig. 7. Variation of the input admittance of an air-insulated monopole with respect to $a_2/a_0$($a_0 = 3.175$ mm, $a_1 = 2.301a_0$, $\epsilon_r^I = 1$, $\epsilon_3 = 4.82$, $a_3 - a_2 = 0.1a_0$, $h = 0.25\lambda_0$, $f = 380$ MHz, $\epsilon_{r4} = 4.82$).

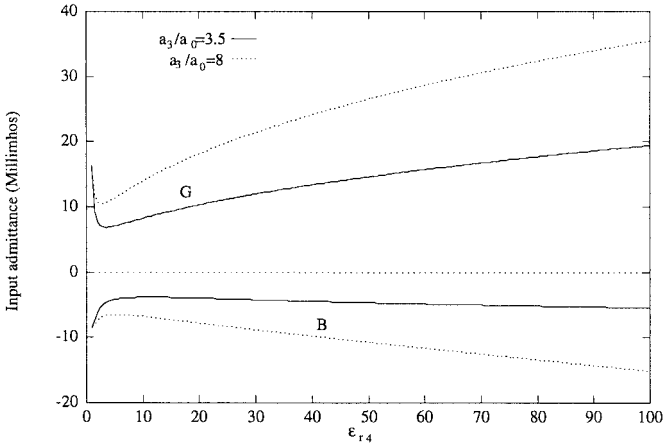


Fig. 8. Variation of the input admittance of an air-insulated monopole with respect to $\epsilon_{r4}$ ($a_0 = 3.175$ mm, $a_1 = 2.301a_0$, $\epsilon_r^I = 1$, $a_3 - a_2 = 0.1a_0$, $h = 0.25\lambda_0$, $f = 380$ MHz, $\epsilon_{r3} = 4.82$).

Lee *et al.* [2], [7]. It is noted that $\exp(j\omega t)$ is used as the time-harmonic factor in this paper, rather than $\exp(-i\omega t)$, which was employed in the previous work; this explains the reason why $-\mathrm{Arg}[I(z)]$ is used in Fig. 5. Agreement is very good with those computed by Lee *et al.* [3]. Both theoretical predictions agree reasonably well with the experimental results [7]. It should be pointed out that our modal-expansion method has no limitation on the monopole radius, relative permittivity, and number of dielectric layers of the insulated monopole antenna. The model we employed can also take the effect of the junction at the monopole base into account, which will be studied in the next subsection.

Fig. 7 shows the variation of the input admittance of an air-insulated monopole with respect to the radius of the insulating layer of zero thickness. Since for the insulated monopole antenna most of the power is radiated in the radial direction, the effect of the permittivity discontinuity between the insulating air and its ambient medium is very similar to a step discontinuity in characteristic impedance of a lossy transmission line. Meanwhile, the radial line is nonuniform; its characteristic impedance decreases very rapidly as the radius increases. Therefore, the curve of the input admittance versus $a_2/a_0$ is somewhat like a fast-decaying standing wave, as illustrated in Fig. 7. Furthermore, since the admittance of an antenna in an infinite homogeneous medium is proportional to $\sqrt{\epsilon_r}$ [18], its magnitude variation will be bigger for higher permittivity of the ambient medium, as seen in Fig. 7.

Fig. 8 gives the input admittance with respect to the relative dielectric constant of the external medium. When the relative permittivity increases, the reflection coefficient at the interface between the insulating layer and the external medium and the antenna's admittance (absolute value) will also increase. Fig. 8 shows this except for small $\epsilon_{r4}$ for which the reflection coefficient is not large enough to dominate the variation.

Finally, we take an air-insulated monopole antenna with an insulating glass layer of finite thickness as an example of a multilayer insulated monopole. Fig. 9 shows the input admittance of the insulated monopole for different layer thicknesses. The thickness of the insulating layer has a significant effect on both the conductance and the susceptance. This is expected since a big difference exists in the relative permittivities of the insulating glass and lake water and this difference changes the equivalent radius of the insulating layer which has a noticeable

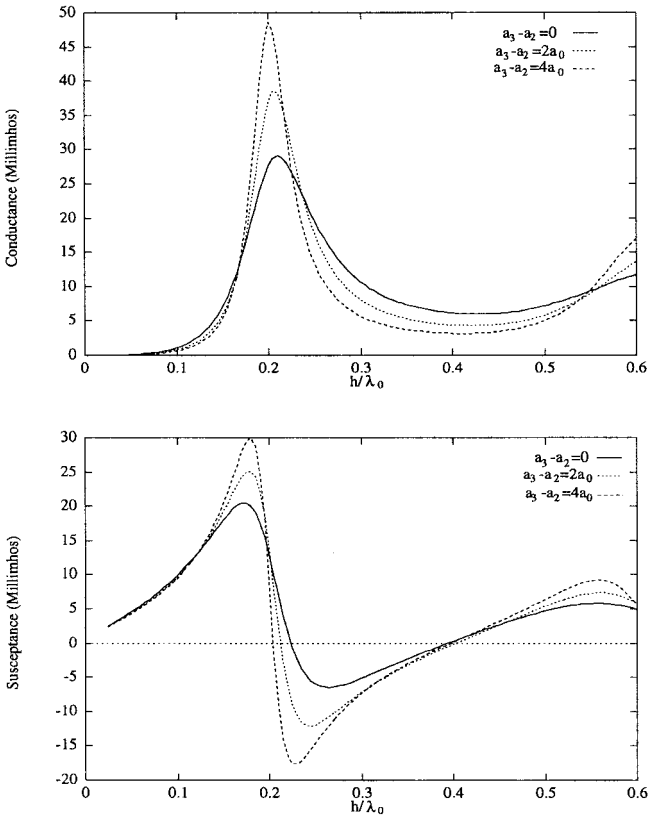


Fig. 9. Effect of the finite thickness of the insulating layer on the monopole's input admittance ($a_0 = 3.175$ mm, $a_1 = 2.301a_0$, $\epsilon_r^I = 1$, $f = 380$ MHz, $a_2 = 4a_0$, $\epsilon_{r3} = 4.82$, $\epsilon_{r4} = 80$).

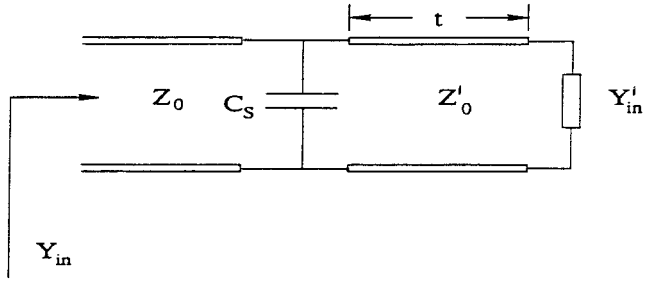


Fig. 10. Equivalent circuit for characterizing the junction effect.

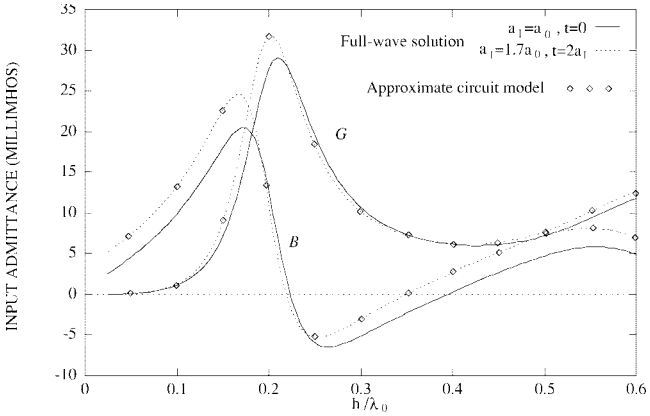


Fig. 11. Effect of the step junction between the monopole and the feed line on an air-insulated antenna's input admittance ($a_0 = 3.175$ mm, $a_1 = 2.301a_0$, $\epsilon_r^I = 1$, $f = 380$ MHz, $a_2 = 4a_0$, $a_3 - a_2 = 0.1a_0$, $\epsilon_{r3} = 4.82$, $\epsilon_{r4} = 80$).

effect on the antenna's admittance (see Fig. 7). The effect becomes negligible for an air-insulated monopole immersed in sand since the difference in the permittivities of glass $(\epsilon_r = 4.82)$ and sand $(\epsilon_r = 3.8)$ is relatively small.

### C. Junction Effect

The effect of the step junction at the end of the monopole is rigorously examined by using the full-wave formulation presented in Section II. In order to gain understanding of this junction effect, we also introduce a simple equivalent circuit model in this subsection. It is well known that a step discontinuity in the inner conductor of a coaxial waveguide can be characterized by a parallel capacitance. For the step junction in the feed line, the capacitance is approximately expressed as [19]

$$C_s = 2a_1\left[\epsilon_1 \frac{\alpha^2+1}{\alpha}\ln\frac{1+\alpha}{1-\alpha} - 2\epsilon_1 \ln\frac{4\alpha}{1-\alpha^2} + 3.487\times 10^{-13}(1-\alpha)(a_1/a_0-1)\right] \quad (13)$$

where $\alpha = (a_1 - b_1)/(a_1 - a_0)$. The input admittance $Y_{\text{in}}$ of the insulated monopole looking from the coaxial feed line is then calculated from the equivalent circuit shown in Fig. 10, where $Y'_{in}$ is the admittance of the monopole at $z = D$, i.e., without the junction effect

$$Y_{\text{in}} = j\omega C_s + [Z'_0 Y'_{\text{in}} + j\tan(k_1 t)]/[Z'_0 + j(Z'_0)^2 Y'_{in}\tan(k_1 t)] \quad (14)$$

where $k_1 = k_0\sqrt{\epsilon_{r1}}$ and $Z'_0$ is the characteristic impedance of the coaxial line whose inner and outer radii are $a_0$ and $a_1$, respectively.

To appreciate the effect of the step junction at the monopole base on the antenna's input admittance and to examine the accuracy of the circuit model, we give a comparison between $Y'_{in}$ and $Y_{in}$ obtained by our modal expansion method and (13) and (14), as illustrated in Fig. 11. It is found that the step junction has a noticeable effect on the antenna's admittance, while it depends on the size of the step junction and the length $t$. The admittance calculated by (13) and (14) agrees very well with the full-wave solution obtained by our modal-expansion method. Since the electrical dimensions of the feed line and the step discontinuity are relatively small, the low-frequency circuit model (13), (14) provides a good estimate of the junction effect.

## IV. Conclusion

This paper has provided a formally exact modal-expansion analysis of the current distribution and input admittance of a multilayer insulated monopole antenna driven through an infinite conducting ground plane from a coaxial line. An efficient recursive algorithm has been introduced to implement the analysis of an arbitrary multilayer insulated monopole antenna. As examples, a dielectric-coated monopole and an air-insulated monopole antenna are considered. Our modal-expansion results for the input admittance of these antennas are compared to the experimental data available in the literature.

Good agreement is achieved. Numerical results for the effect of the thickness of the insulated layer are presented and discussed. Finally, the junction effect of a step discontinuity between the monopole radius and that of the inner conductor of the coaxial feed line is considered.

## APPENDIX

The elements of the matrices occurring in (9)–(11) can be worked out [20] as follows:

$$W_{Amn} = \frac{4\epsilon_1}{LD\epsilon_2} F_{mn}(D)$$
$$W_{Bmn} = F_{mn}(d) \frac{4\epsilon_1 \gamma_n^{II} J_0\left(\gamma_n^{II} a_0\right)}{Ld\epsilon^{II} J_1\left(\gamma_n^{II} a_0\right)} \tag{A.1}$$

$$W_{Cmn} = j2\pi\omega\epsilon_1 \int_{b_1}^{a_1} e_{1m\rho}(\rho) e_{In\rho}(\rho) \rho \, d\rho$$
$$M_{ICmn} = \frac{\sin(\alpha_n L)}{j\omega\epsilon_1 \alpha_n \cos(\alpha_n L)} W_{Cnm} \tag{A.2}$$

$$M_{2Amn} = -F_{nm}(d) \frac{U'_{1n}(a_0)}{\gamma_{1n}^2}$$
$$M_{2Bmn} = -F_{nm}(d) \frac{V'_{1n}(a_0)}{\gamma_{1n}^2} \tag{A.3}$$

$$M_{3Amn} = -F_{nm}(D) \frac{U'_{1n}(a_1)}{\gamma_{1n}^2}$$
$$M_{3Bmn} = -F_{nm}(D) \frac{V'_{1n}(a_1)}{\gamma_{1n}^2} \tag{A.4}$$

$$M_{2Cmn} = e_{1n\rho}(a_0) S_{mn}(d)$$
$$M_{IAmn} = \frac{2\pi(-1)^n}{\gamma_{1n}^2} \int_{b_1}^{a_1} e_{Im\rho}(\rho) U'_{1n}(\rho) \rho \, d\rho \tag{A.5}$$

$$M_{3Cmn} = e_{1n\rho}(a_1) S_{mn}(D)$$
$$M_{IBmn} = \frac{2\pi(-1)^n}{\gamma_{1n}^2} \int_{b_1}^{a_1} e_{Im\rho}(\rho) V'_{1n}(\rho) \rho \, d\rho \tag{A.6}$$

$$Y_{An} = -\frac{D[U'_{2n}(a_1) R_{Tn} + V'_{2n}(a_1)]}{2\gamma_{2n}^2} \tag{A.7}$$

where

$$F_{mn}(x) = \int_0^x \sin\frac{(2m+1)\pi z}{2L} \sin\frac{(2n+1)\pi z}{2x} \, dz$$
$$S_{mn}(x) = \int_0^x \frac{-\sin(\alpha_n z)}{\alpha_n \cos(\alpha_n L)} \sin\frac{(2m+1)\pi z}{2x} \, dz.$$

## REFERENCES


[1] R. W. P. King and G. S. Smith, *Antennas in Matter: Fundamentals, Theory and Application*. Cambridge, MA: MIT Press, 1981.

[2] K. M. Lee, "Insulated linear antenna," in *Research Topics in Electromagnetic Wave Theory*, J. A. Kong, Ed.. New York: Wiley, 1981, pp. 235–263.

[3] T. T. Wu, R. W. P. King, and D. V. Giri, "The insulated dipole antenna in a relatively dense medium," *Radio Sci.*, vol. 8, pp. 699–709, 1973.

[4] R. W. P. King, K. M. Lee, S. R. Mishra, and G. S. Smith, "Insulated Linear antenna: Theory and experiment," *J. Appl. Phys.*, vol. 45, pp. 1668–1697, Apr. 1974.

[5] R. W. P. King, K. M. Lee, G. S. Smith, and S. R. Mishra, "Insulated Linear antenna: Theory and experiment II," *J. Appl. Phys.*, vol. 46, pp. 1091–1098, Mar. 1975.

[6] R. W. P. King, S. R. Mishra, K. M. Lee, and G. S. Smith, "The insulated monopole: Admittance and junction effects," *IEEE Trans. Antennas Propagat.*, vol. AP-23, pp. 172–177, Feb. 1975.

[7] K. M. Lee, T. T. Wu, and R. W. P. King, "Theory of an insulated linear antenna in a dissipative medium," *Radio Sci.*, vol. 12, pp. 195–203, 1977.

[8] K. Lamensdorf, "An experimental investigation of dielectric-coated antennas," *IEEE Trans. Antennas Propagat.*, vol. AP-15, pp. 767–771, June 1967.

[9] C. Y. Ting, "Theoretical study of finite dielectric-coated cylindrical antenna," *J. Math. Phys.*, vol. 10, no. 3, pp. 480–493, Mar. 1969.

[10] J. H. Richmond and E. H. Newman, "Dielectric coated wire antennas," *Radio Sci.*, vol. 11, no. 1 pp. 13–20, 1976.

[11] B. P. Sinha and S. A. Saoudy, "Rigorous analysis of finite length insulated antenna in air," *IEEE Trans. Antennas Propagat.*, vol. 38, .pp. 1253–1258, Aug. 1990.

[12] Z. Shen and R. H. MacPhie, "Modal expansion analysis of monopole antennas driven from a coaxial line," *Radio Sci.*, vol. 31, no. 5, pp. 1037–1046, 1996.

[13] ———, "Rigorous evaluation of the input impedance of a sleeve monopole by modal expansion method," *IEEE Trans. Antennas Propagat.*, vol. 44, n pp. 1584–1591, Dec. 1996.

[14] M. A. Morgan and F. K. Schwering, "Eigenmode analysis of dielectric loaded top-hat monopole antennas," *IEEE Trans. Antennas Propagat.*, vol. 42, pp. 54–63, Jan. 1994.

[15] N. Marcuvitz, *Waveguide Handbook*. New York: McGraw-Hill, 1951.

[16] E. Kuhn, "A mode-matching method for solving field problems in waveguide and resonator circuits," *Arch. Elek. Ubertragung.*, vol. 27, pp. 511–518, Dec. 1973.

[17] R. Mittra and S. W. Lee, *Analytical Techniques in the Theory of Guided Waves*. New York: Macmillan, 1971.

[18] R. W. P. King, *The Theory of Linear Antennas*. Cambridge, MA: Harvard Univ. Press, 1956.

[19] P. I. Somlo, "The computation of coaxial line step capacitances," *IEEE Trans. Microwave Theory Tech.*, vol. MTT-15, no. 1, pp. 48–53, Jan. 1967.

[20] M. Abramowitz and I. A. Stegun, *Handbook of Mathematical Functions*. New York: Dover, 1965.



**Zhongxiang Shen** (S'96) was born in Zhejiang Province, China, in 1966. He received the B.E. degree in electromagnetic engineering from the University of Electronic Science and Technology of China, Chengdu, China, in 1987, the M.S. degree in radio engineering from Southeast University, Nanjing, China, in 1990, and the Ph.D. degree in electrical engineering from the University of Waterloo, Waterloo, ON, Canada, in 1998.

From 1990 to 1994, he was with Nanjing University of Aeronautics and Astronautics, China, and from 1994 to 1997, he was a Research and Teaching Assistant with the Department of Electrical and Computer Engineering, University of Waterloo. He worked for ComDev Ltd., Cambridge, ON, Canada, as an Advanced Member of Technical Staff for eight months in 1997. He is currently a Postdoctoral Fellow at Gordon McKay Laboratory, Harvard University, Cambridge, MA. His current interests include modeling of passive microwave and millimeter wave components, microstrip circuits and antennas, and linear antennas.

**Robert H. MacPhie** (S'57–M'63–SM'79–F'91) received the B.A.Sc. degree in electrical engineering from the University of Toronto, Toronto, ON, Canada, in 1957, and the M.S. and Ph.D. degrees from the University of Illinois, Urbana, IL, in 1959 and 1963, respectively.

In 1963, he joined the University of Waterloo, Waterloo, ON, Canada, as an Assistant Professor (electrical engineering) where he is now Adjunct Professor of electrical and computer engineering. From 1991 to 1992 he was on sabbatical leave as a Professeur Associé at the University of Aix-Marseille I, France, working in the Département de Radioélectricité. His current research interests focus on waveguide scattering theory, scattering from spherical bodies, and linear antennas.